LEMUR 3: A Limbed Climbing Robot for Extreme Terrain Mobility in Space

Aaron Parness[1], Neil Abcouwer, Christine Fuller, Nicholas Wiltsie, Jeremy Nash, Brett Kennedy

***Abstract*— This paper introduces a new four-limbed robot, LEMUR 3, that has demonstrated climbing on cliff faces and smooth glass. Each limb on the robot consists of seven identical actuators in a serial chain. Each limb terminates in a single axis force sensor that allows various end effectors to be mounted and connected to the robot's power and communication system. Microspine grippers were used for climbing the rocky surface and gecko adhesive grippers were used for the glass solar panels. All other hardware and much of the software was common for the two demonstrations. The robot's mechanical, electrical, and software systems, various gripping devices, and field demonstrations are described. Limbed mobility is of interest to JPL and NASA because of its potential to access extreme terrain, including that on Mars and in microgravity environments.**

I. Introduction

Three generations of wheeled robots have explored Mars [1]–[3] and three types of wheeled robots have driven on the Moon [4]–[6]. The objectives of these missions were enabled by the mobility of these vehicles. However, several terrain types with high scientific value are not accessible to wheeled systems, and several incidents have shown the vulnerabilities of wheeled architectures. For example, the Opportunity Rover observed layering in the rock outcrops at Victoria Crater. Like the layers we see in our Grand Canyon, these stratified sedimentary layers can allow us to see back in time and understand the geologic history of the site. Despite the efforts of the rover drivers, Opportunity could not reach the layering to deploy its scientific instruments because the slopes were too steep [7]. The twin Spirit rover had the unfortunate fate of getting stuck in loose sand and was unable to free itself, due in part to the limited degrees of freedom of its wheeled architecture [8]. Most recently, the Curiosity rover has suffered from punctures in its wheels that have slowed its progress and limited terrain types that could be traversed [9].

On flat terrain, the efficiency benefits of wheels are clear, but limbed robots can maneuver across rougher terrains. This can include steep slopes and even vertical cliff faces. On Mars, these are some of the most scientifically interesting targets due to the layering and the observation of seasonal liquid water seeps [10]. When equipped with gripping end effectors, limbed robots also have the potential to enter and explore caves (including the cave ceilings) whose entrances have been observed from orbit [11], or traverse microgravity bodies like asteroids, comets, and small moons where there is insufficient ground pressure for wheeled robots to obtain traction. Limbs can also double as a manipulation system. Spirit, Opportunity, and Curiosity all used a separate limb to place instruments on the surface.

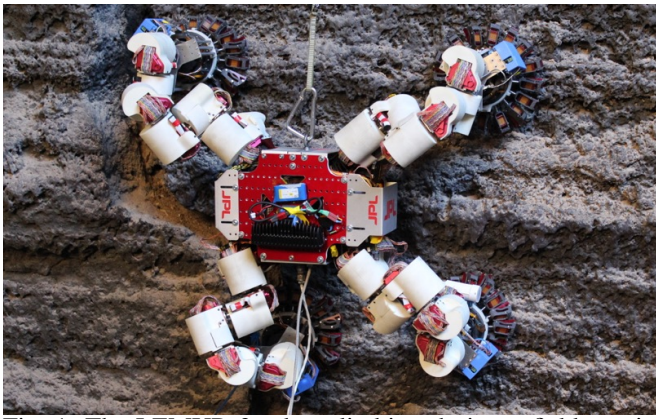

Fig. 1: The LEMUR 3 robot climbing during a field test in a lava tube. Extreme terrains with high scientific value like exposed stratified sedimentary rock on cliff walls have been previously inaccessible to robotic space missions.

In low gravity environments, hopping robots have also been proposed, but the propellant used by hopping robots is an expendable resource that limits operation. On many small moons, asteroids, and comets, hopping robots also face the real danger of reaching escape velocity, and their flight is often complicated by orbital dynamics and complex gravity fields that prevent simple flight planners. In complete microgravity environments like the outside of the International Space Station, limbed robots with gripping end effectors have the same advantages over free-flying robots. Limbed robots can crawl across surfaces, place inspection instruments precisely, and react contact loads that common non destructive evaluation instruments require, all without consuming expendable resources like propellant.

The biggest drawback to limbed robots is their complexity. This leads to higher cost and higher risk of failure in some cases, although the redundancy and adaptability of limbs can overcome failures that simpler architectures may suffer. There has been considerable progress in limbed robot design and reliability. Multiple limbed robots from Boston Dynamics have demonstrated tremendous stability and robustness to outside disturbances and challenging terrain types [12,13]. The DARPA Robotics Challenge [14] and other efforts [15,16] have showcased many advances in mobility and manipulation using a variety of limbed system designs. JPL has been developing limbed robots for planetary exploration

[1]Jet Propulsion Laboratory, California Institute of Technology Aaron.Parness@jpl.nasa.gov

and spacecraft inspection at multiple sizes for the past two decades. These systems include ATHLETE [17,18] at the 1000 kg scale, RoboSimian [19] at the 100 kg scale, and LEMUR 1, LEMUR 2A, and LEMUR 2B [20] at the 10 kg scale. LEMUR 3 is the largest and most versatile platform in the series of LEMUR robots. Its design was motivated by a desire to climb arbitrary geometries, leading to a 7 degree of freedom per limb approach. This approach enables the robot to maneuver across curved walls, large obstacles, and corners (plane-changes). A comparison of these limbed platforms is shown in table I.

This paper presents the LEMUR 3 robot. LEMUR 3 was built for two projects, one focused on crawling across the exterior of the International Space Station using gecko adhesive end effectors [22], and one focused on climbing vertical cliffs and traversing cave ceilings on the Moon and Mars using microspine grippers [23]. Because walking in microgravity is functionally equivalent to climbing (if the robot does not grip the surface, it will fall off), the autonomy and perception systems for these two projects are largely common. In fact, because the limbs of the robot can interface with any number of grippers, configuring LEMUR 3 to climb across the icy terrain of Enceladus or over the granular surface of a comet would only require switching the end effector.

II. Mechanical Design

The LEMUR 3 robot consists of a central body, four 7-DOF limbs, and four grippers at the ends of the limbs. Originally, all 28 actuators comprising the limbs were identical, allowing for reduced design complexity, reduced fabrication costs (through low unique part count), and easier repair and replacement of components, similar to the RoboSimian robot [19]. Later, the first joint (shoulder) of each limb was upgraded with a motor with a higher reduction gearbox to provide more torque capacity, but retained the same gearbox design.

However, LEMUR 3's joint configuration results in non-intuitive kinematics. Because each LEMUR 3 joint has a non-zero link length, no three joint axes intersect. This precludes spherical joint decoupling that can simplify inverse kinematics to have closed form solutions.

A. Actuator Design

A cross-sectional view of a single actuator is shown in Figure 2. Each actuator has two major fabricated parts: an aluminum housing and a steel output drive shaft. The distal end of each output shaft is bolted to the flat face of the next actuator's housing, resulting in a 90-degree twist between adjacent actuators, see Figure 3.

A cross-axis roller bearing mounted into the housing constrains the output shaft to a single rotational degree of freedom. Using a single cross-axis roller bearing rather than a duplex pair of tapered needle bearings allows for a substantial reduction in the actuator mass.

In addition to the motor's incremental encoder, each actuator includes an AMS AS5040 absolute magnetic encoder to measure the position of the output shaft. A radially-polarized rare-earth magnet is adhered to the tip of the output shaft; the encoder and PCB are mounted to the housing cap.

Each actuator includes a 3D-printed cover to protect the electrical harnesses, cable connectors, and other electrical components. The harnesses are composed of 28 AWG twisted-pair ribbon cables, with one connectorized cable assembly per actuator. Each harness is wrapped twice around the output shaft, allowing for a 360-degree range of motion for the actuator as the harness unspools and fills the volume of the twist capsule.

B. Actuator Sizing and Drivetrain

The CSF-11 harmonic drive gears used in the LEMUR 3 actuators have a rated ratchet torque (the torque at which the spline teeth will slip) of 40 N-m. As the full mass of the limb is carried by the first joint during a step, and a fraction of the combined mass of the robot and limbs are carried by the furthest joint while standing, this 40 N-m maximum load limits the mass of the robot and determined the total gear ratio. Each motor and output shaft are connected through a 5.4:1 planetary gearbox, a 2.24:1 single-stage spur gear pass, and a 100:1 CSF-11 harmonic drive for a total 1209.6:1 gear ratio with a 5.5 N-m continuous torque and a 43.9 N-m stall torque (slightly higher than the rated ratchet torque of the harmonics). The first (proximal) joint in each limb carries the largest load and, to accommodate, has a larger planetary gear reduction than the other joints (19:1 versus 5.4:1), with a 19.3 N-m continuous torque and a 115.5 N-m stall torque.

In each actuator, the spur gear pinion is clamped to the motor shaft, while the drive gear is concentrically bolted to the harmonic's wave generator. The drive gear and wave generator are constrained by a pair of ball bearings to be concentric to the output shaft. The harmonic's flexible spline is pinned and bolted to the shoulder of the output shaft.

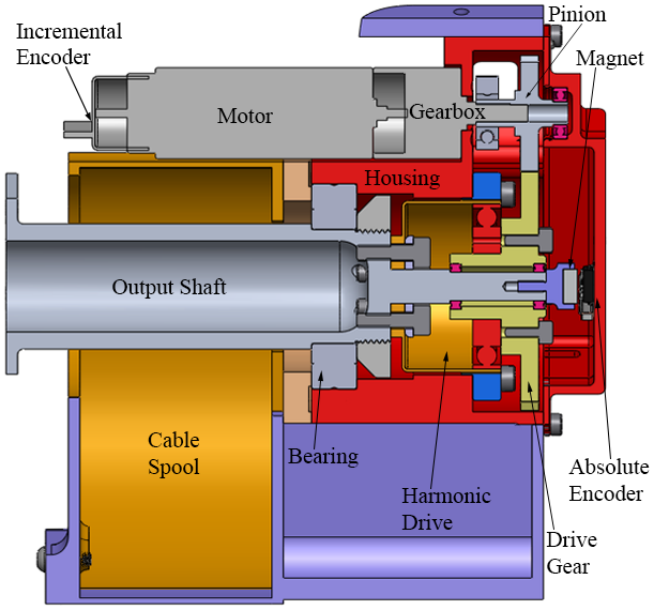

Fig. 2: Cross-sectional view of an actuator.

TABLE I: Comparison of Limbed Robots Developed at JPL

Robot	Year	DOF per limb	limbs	Mass (kg)	Track[1] (m)	Step Size (m)	End Effector(s)
LEMUR 1	2000	3/4[2]	6	5	0.35	0.05	Quick Release Tools
LEMUR 2A[3]	2001	4	6	15	0.76	0.1	Quick Release Tools
LEMUR 2B	2005	3	4	12	1.0	0.30	Tools or Microspine Grippers
LEMUR 3	2015	7	4	35	0.8	0.10	Microspine, Gecko, or Ice Screw Grippers
RoboSimian	2014	7	4	134	1.10	0.40	Cam Hand
ATHLETE	2005	6	6	850	∼3.3	>0.75	Wheels, Foot Pad, or Tools.
Tri-ATHLETE	2010	7	6	∼1600	∼7	>1.5	Wheels, Foot Pad, or Tools

1 Track refers to the distance between grippers during the robot's natural locomotion; i.e. instantaneous wingspan during nominal climbing gait
2 LEMUR 1 had 3 DOF for its four rear limbs and 4 DOF for the front two.
3 Upgraded in 2013 [21] with Elmo motor controllers. Upgraded mass reported.

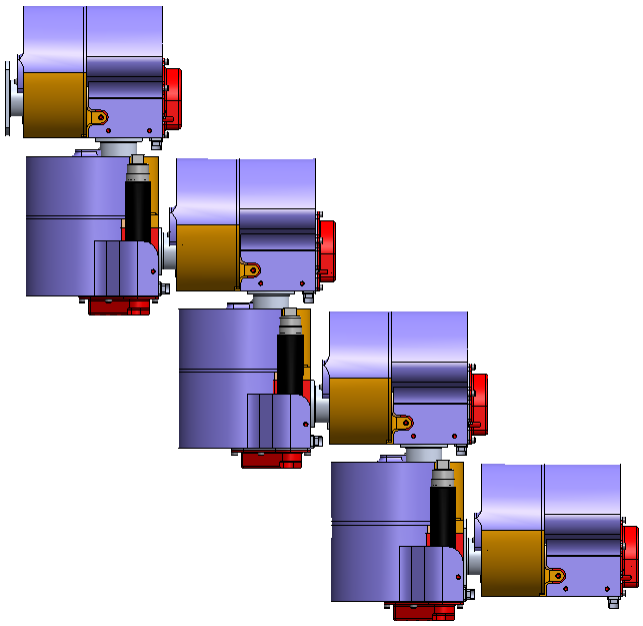

Fig. 3: Rendering of a single limb.

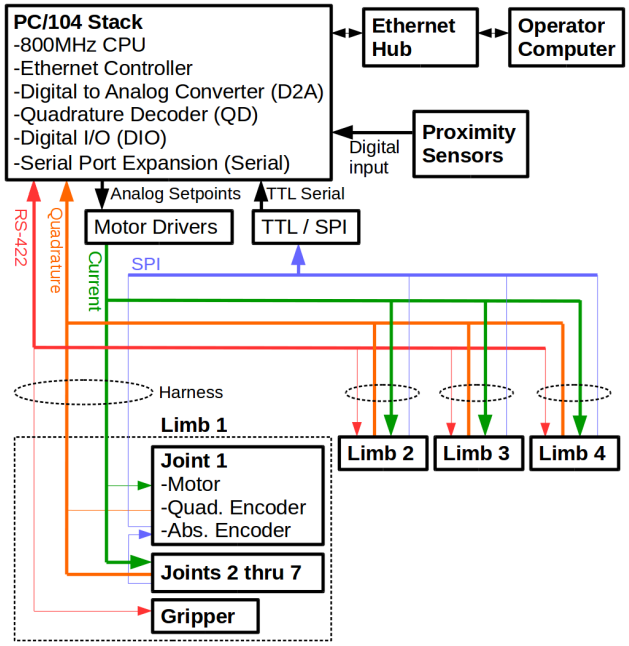

Fig. 4: Functional block diagram for LEMUR 3 electronics. Limb 1 is exploded for detail. Pointers indicate input/output relationships. Bold lines indicate multiple channels of protocol. Power distribution is omitted for clarity.

III. Electrical Design

The heart of the LEMUR 3 electrical design is the "stack," a centralized PC/104 computer system in the chassis, which includes a CPU module, power conversion, and various interface boards on a PC/104 bus, as shown in Figure 4. Power is delivered via tether, which includes an Ethernet connection.

Four limbs are connected to the chassis, and each limb consists of seven identical joints and a gripper (detailed in Section V). Running the length of the limb is a limb harness, connecting each motor, quadrature encoder, and gripper to the stack. The absolute encoders are configured in a daisy chain, where each encoder reports its own position and positions received from the next distal encoder via SPI, and the SPI communication is converted to TTL serial for the stack. Each joint is controlled with coordination between the various interface boards. Absolute encoders are used to determine the initial position of each joint, which is later tracked by quadrature encoder. The D2A board provides analog set points to motor drivers, which excite the motors. Additionally, digital proximity sensors are used to gauge proximity between the chassis and the climbing surface.

IV. Software

The LEMUR 3 software runs on an 800Mhz VDX-6354 PC/104-compatible CPU board running a QNX real-time operating system and is primarily written in C. The software employs a layered architecture, broken into driver, device, application, and system layers, see Figure 5. A user interface on a separate computer issues commands to the robot.

A. Architecture

1) Driver Layer: The driver layer consists of driver code for each interface board on the PC/104 stack.

2) Device Layer: The device layer abstracts individual drivers and represents the robot subsystems, including the grippers, proximity sensors, and limb joints. Grippers and proximity sensors are primarily wrappers around drivers, but limb motion requires position tracking, PID control, trajectory generation, and smoothing between trajectories in

a queue. Reliable motor control drives the selection of the real-time operating system.

3) Application Layer: The application layer is responsible for handling inverse kinematics (IK) and complex commands that require planning and coordinated actuation over an extended period of time. These commands include Cartesian motion, coordinated limb and gripper control, and sequences that generate gait cycles and mobility, discussed below.

4) System Layer: The system layer is responsible for managing all the periodic tasks of the system and network communication with the user interface. Tasks can be run more or less frequently depending on their criticality. Motor control runs at 512Hz.

5) User Interface: A user may send individual commands or sequences and monitor results and status via GUI.

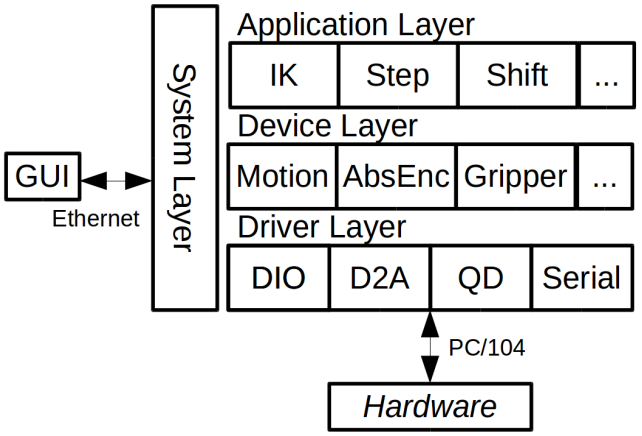

Fig. 5: The LEMUR 3 software employs a layered architecture. The driver layer communicates over the PC/104 bus to hardware, the device layer encapsulates the drivers and represents subsystems, the application layer manages high-level, multi-subsystem tasks, and the system layer maintains control loops and communicates with the user interface.

B. Operation

LEMUR 3 mobility is achieved by repeating a gait, which consists of coordinated steps and body shifts using the limbs and grippers. To step, one gripper is first released and moved away from the surface, typically along the surface normal. The gripper is then moved a new desired position, offset above the surface. It is then lowered to the surface along the new surface normal. To ensure firm contact, a gripper preload can be applied and measured by a single axis force sensor on the each gripper. When sufficient contact force is reached the gripper is engaged. After a successful grip, the preload is relieved.

Planning limb motions in Cartesian space, rather than joint space, requires solving the inverse kinematics (IK) problem. Some robot manipulators are designed to simplify IK, often with a spherical wrist for resolving orientation and three or more joints for resolving position. However, LEMUR 3's limbs consist of identical joints in a chain, and because no three joint axes intercept, no spherical joints can be represented. OpenRAVE's [24] ikfast module was used to generate code that gives IK solutions. Given a desired end effector pose and a position for the seventh "free" joint, this solver returns a list of solutions for the remaining six joints, if solutions exist. To generate smooth joint trajectories, the LEMUR 3 software tests a range of free joint positions and chooses the collision-free solution closest to a desired default posture or the previous solution in the trajectory.

Once all four limbs have stepped forward, a body shift is executed by moving the end effectors simultaneously relative to the body frame. Body shifts can also be used in conjunction with proximity sensors to move the body frame towards and away from the surface to focus attached science instruments. This was demonstrated with a near infrared spectrometer in the field [25]. "Neutral" body shifts can also be used to center the body between the end effectors to increase manipulability before engaging in data gathering motions or transitioning to a new direction of travel.

Step and body shift commands together form a gait that can be repeated to move the robot along a surface. During the last field test, a human operator observed the robot on the wall and determined desired gripping poses and the robot's direction of travel. The operator avoided obstacles that were too large to step over and favored surface normals that aligned with the robot's body. Ongoing work (Section VII) involves automating this behavior by creating both a perception system for understanding the climbing surface and a planning system for gripper emplacement, gait sequencing, and robot-level path planning.

V. Grippers

LEMUR 3 has been demonstrated climbing on smooth surfaces with gecko adhesive grippers and on rock surfaces using microspine grippers. The robot is designed to easily accept future end effectors that may be designed for other surfaces, such as ice or granular media. The grippers are operated by a microcontroller and two motor drivers. The gripper mechanically interfaces to a single axis load cell, primarily used to determine when grippers makes contact with the surface. Each gripper receives power and RS-422 serial commands from the PC/104 stack. Commands from the stack are high level (e.g. attach, check force). This versatile architecture and command interface allows common use of the perception system and mobility software.

A. Gecko Adhesive Grippers

LEMUR 3 uses gecko adhesive grippers to climb on smooth, flat, clean surfaces including glass as previously demonstrated by several simpler and lighter robots [26]–[28]. Geckos climb using microscopic hairs (setae) that adhere by van der Waals forces. Previous work developed a synthetic gecko adhesive [29], creating 80 μm hairs out of silicone. When the material is placed on a flat surface and sheared in the attach direction, the hairs comply to the surface creating a large area of contact with minimal stored energy. Van der Waals forces cause an attraction between the adhesive and the surface, attaching the gripper. When the gripper is sheared

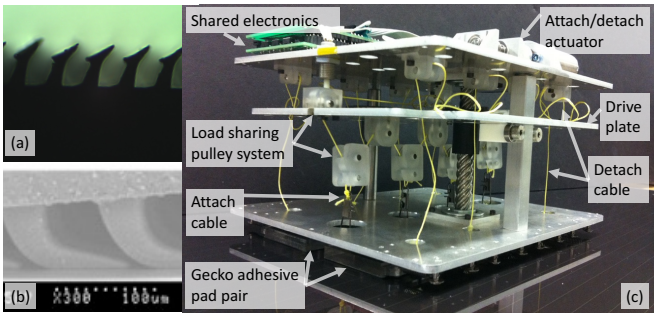

Fig. 6: Gecko adhesive in its detached state (a) and its attached state (b). Gecko adhesive gripper (c) attached to a solar panel.

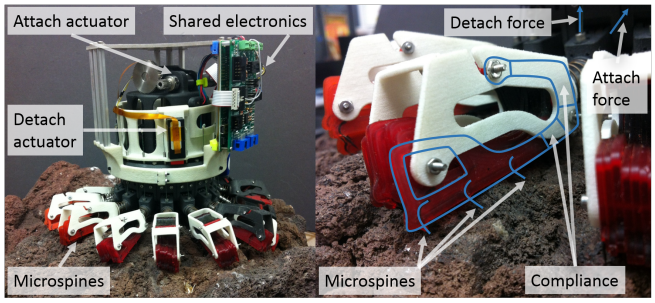

Fig. 7: Microspine gripper attached to vesicular basalt (left). Close-up of one microspine carriage, with the outline of one toe labeled to show compliant sections (right).

in the detach direction, the hairs are peeled up, real area of contact and van der Waals forces are lost, and the gripper detaches with very low force. In this way, the gecko adhesive can be turned on and off. Adhesive performance for this class of materials usually degrades significantly with dirt, high surface roughness, or if the material is wet.

LEMUR 3 gecko adhesive grippers can support a normal load of 150 N using eight 10 cm^2 tiles of adhesive. The tiles are arranged in opposing pairs. Pulling on a cable between the pairs attaches the gripper. Separate cables connected to the back of each pad detach them. A single motor drives both the attaching and detaching cables by moving a plate of pulleys up and down. The pulleys share load equally between the pads [30].

B. Microspine Grippers

LEMUR 3 traverses rock faces using four microspine grippers. Hundreds of hooks on flexible suspension structures, called microspines [31], are pulled across the rock towards the center of the gripper. Hierarchical compliance allows each hook to conform to the surface at multiple scales [32]. Individual microspines conform to mm-scale roughness while carriages of 16 microspines conform at the cm-scale. A series of flexible elements allows microspines that catch in asperities to bear load while neighboring microspines continue to move. Only a small fraction of microspines need to adhere for a successful grip. Each gripper has a 23 cm diameter and can support 150 N on vesicular basalt, commonly found in lava tubes and on flow fields. This technology was demonstrated on several previous, simpler robots [23,33,34].

VI. Test Results and Discussion

The LEMUR 3 robot was tested on both natural rock surfaces and a smooth solar panel surface using microspine and gecko-adhesive grippers, respectively. These two demonstrations used largely the same control software and no hardware differences other than the end effectors. LEMUR 3's serial joint limb kinematics showed the ability to step over obstacles (solar panel demonstration) and conform to varied natural roughness (cliff face demonstration). To replicate the reduced-gravity or zero-gravity environment of each mobility scenario, the robot was gravity offloaded in both types of tests using an overhead constant force spring. Neither set of grippers is sufficient to support LEMUR 3's mass in Earth's gravity under all conditions.

Gecko adhesive mobility tests were performed at JPL with a full-weight gravity offload on a mock-solar panel surface to simulate the exterior of the International Space Station. Traverses of 0.25 m were performed in cardinal and diagonal directions relative to the limbs, and traversing over obstacles (eg. handrails) and simple manipulation tasks were demonstrated. These results are shown in Figure 8 and in the supplementary video.

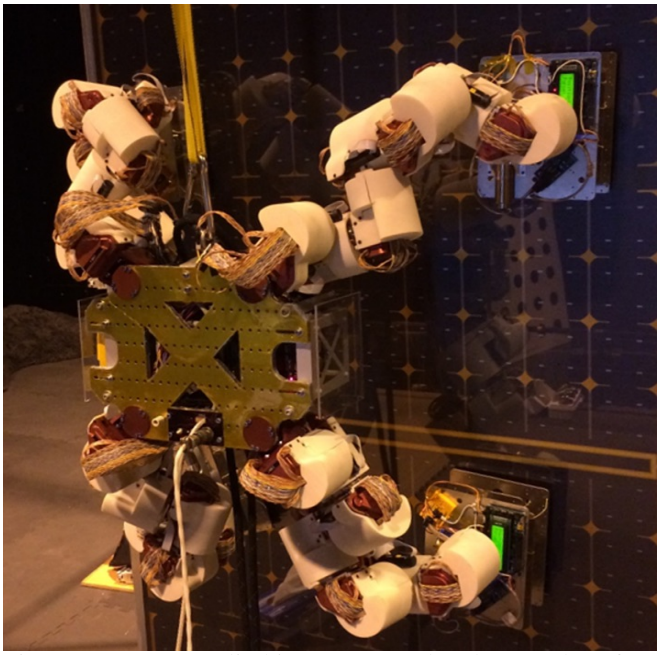
Fig. 8: LEMUR 3 climbing on a mock-solar panel surface using gecko adhesive grippers.

A rock climbing demonstration was performed in Big Skylight Cave at El Malpais National Monument, New Mexico, see Figure 9. El Malpais provides a variety of terrain features and gravitational orientations to test the robot, making it a good analog for microgravity surfaces and for lava tubes on Mars and the Moon. LEMUR 3 successfully climbed 0.8m of a rock face with a traverse rate of 0.16 m/hr using

microspine grippers. The speed of the robot was limited by a slow gripping sequence, which took approximately 3 minutes per grip/ungrip cycle, and further slowed by the lack of autonomy, which required a human operator to specify gripping poses and direction of travel for each step. The grip/ungrip time has been subsequently shortened to 20 seconds by replacing the gripper motors and improved software is in development to autonomously climb towards a given target.

VII. Future Work

The LEMUR 3 robot is a prototype of a future system that would explore remote sites in space where teleoperation is impeded by long communication delays and poor bandwidth. Ongoing work is focused on developing autonomous mobility to reduce the burden on human operators, increase traverse rates, and improve reliability. Towards that end, we have added a separate, miniature computer (Intel NUC) that communicates with the PC/104 stack to support high-level perception and autonomous planning behaviors performed in ROS. To improve hardware reliability, we also have replaced the ribbon cable electrical harnesses with flex circuit. By bonding the conductors in a dielectric film, the flex circuit harness is significantly more robust and able to survive many thousands of joint rotations. The harnesses are identical for each joint.

A perception system has been constructed, consisting of local gripper-level sensing and body-level sensing to support planning, control, and remote operator awareness. At the gripper level, a ring of infrared depth sensors estimates the distance of the gripper to the surface, while a force-torque sensor in the wrist detects gripper contact and grasping events. At the body level, an illumination-invariant actuated lidar system for reconstructing centimeter-scale geometry that extends from between the limbs up to tens of meters from the robot has been demonstrated. The sensor data is probabilistically aggregated into a persistent 3D occupancy grid, where map patches are evaluated for graspability based on a classifier trained on previous grasping experiences. The geometry can also be queried for collision avoidance for the planning system.

The planning system is similarly hierarchical, consisting of a local footstep planner and a global body-level planner. The global body-level planner evaluates future body positions using a search-based planner across the observed geometry to plan multiple gait-cycles ahead. The local footstep planner uses motion primitives with online adjustments to plan future gripper locations. It also uses closed-loop feedback from the gripper-mounted depth sensors and a contact-triggered state machine to close in on the grasping surface.

Future field tests of the robot will utilize the perception system and increased autonomy to demonstrate faster traverse rates and more complex terrains with less operator intervention. A suite of scientific instruments is also in development that will be deployed from the robot to simulate a mission that would assess habitability and geologic history by transecting a cliff face. A traverse rate of 0.5 to 1.0 m/hr is anticipated for missions to Mars, Asteroids, or other planetary bodies. Higher traverse rates are potentially viable at the International Space Station where the environment is known and power is more readily available.

Fig. 9: The El Malpais field site has multiple types of rocky terrain for testing, and has access to rigging locations for the the gravity offload device and safety harnesses.

In summary, this work presents the design and early field results for a new 7 degree-of-freedom per limb, self-anchoring robot that has cross-cutting applications in space.

ACKNOWLEDGMENT

Research carried out at the Jet Propulsion Lab, California Institute of Technology, under contract with the National Aeronautics and Space Administration.

References

[1] R. Team, "Characterization of the martian surface deposits by the mars pathfinder rover, sojourner," *Science*, vol. 278, no. 5344, pp. 1765–1768, 1997.

[2] R. A. Lindemann and C. J. Voorhees, "Mars exploration rover mobility assembly design, test and performance," in *2005 IEEE International Conference on Systems, Man and Cybernetics*, vol. 1, pp. 450–455, IEEE, 2005.

[3] J. Grotzinger et al., "Mars science laboratory mission and science investigation," *Space science reviews*, vol. 170, no. 1-4, pp. 5–56, 2012.

[4] N. C. Costes, J. E. Farmer, and E. B. George, "Mobility performance of the lunar roving vehicle: terrestrial studies: Apollo 15 results," *NASA Technical Reports Server*, no. R-401, 1972.

[5] S. Kassel, "Lunokhod-1 soviet lunar surface vehicle," tech. rep., DTIC Document, 1971.

[6] W.-H. Ip, J. Yan, C.-L. Li, and Z.-Y. Ouyang, "Preface: The chang'e-3 lander and rover mission to the moon," *Research in Astronomy and Astrophysics*, vol. 14, no. 12, p. 1511, 2014.

[7] S. Squyres et al., "Exploration of victoria crater by the mars rover opportunity," *Science*, vol. 324, pp. 1058–1061, 2009.

[8] Arvidson, RE et al., "Spirit mars rover mission: Overview and selected results from the northern home plate winter haven to the side of scamander crater," *Journal of Geophysical Research: Planets*, vol. 115, no. E7, 2010.

[9] E. Lakdawalla, "Curiosity wheel damage: The problem and solutions," *Planetary Society Blog*, vol. May, 2015.

[10] A. McEwen et al., "Seasonal flows on warm martian slopes," *Science*, vol. 333, pp. 740–743, 2011.

[11] G. Cushing, T. Titus, J. Wynne, and P. Christensen, "Themis observes possible cave skylights on mars," *Geophysical Research Letters*, vol. 34, 2007.

[12] M. Raibert et al., "Bigdog, the rough-terrain quadruped robot," in *Proceedings of the 17th World Congress*, vol. 17, pp. 10822–10825, Proceedings Seoul, Korea, 2008.

[13] G. Nelson et al., "Petman: A humanoid robot for testing chemical protective clothing," vol. 30, pp. 372–377, 2012.

[14] E. Ackerman and E. Guizzo, "Darpa robotics challenge: Amazing moments, lessons learned, and what's next," *IEEE Spectrum*, 2015.

[15] A. Ramezani, J. W. Hurst, K. A. Hamed, and J. Grizzle, "Performance analysis and feedback control of atrias, a three-dimensional bipedal robot," *Journal of Dynamic Systems, Measurement, and Control*, vol. 136, no. 2, p. 021012, 2014.

[16] C. Borst, T. Wimböck, F. Schmidt, M. Fuchs, B. Brunner, F. Zacharias, P. R. Giordano, R. Konietschke, W. Sepp, S. Fuchs, *et al.*, "Rollin'justin-mobile platform with variable base.," in *ICRA*, pp. 1597–1598, 2009.

[17] B. Wilcox et al., "Athlete: A cargo handling and manipulation robot for the moon," *Journal of Field Robotics*, vol. 24, pp. 421–434, 2007.

[18] M. Heverly, J. Matthews, M. Frost, and C. Quin, "Development of the tri-athlete lunar vehicle prototype," *40th Aerospace Mechanisms Symposium*, May 2010.

[19] S. Karumanchi, et al, and B. Kennedy, "Team robosimian: Semi-autonomous mobile manipulation at the 2015 darpa robotics challenge finals," *Journal of Field Robotics: Special Issue on the 2015 DARPA Robotics Challenge Finals*, 2016.

[20] B Kennedy et al., "Lemur iib: A robotic system for steep terrain access," *Industrial Robot: An International Journal*, vol. 33, pp. 265–269, 2006.

[21] D. Helmick, B. Douillard, and M. Bajracharya, "Small body surface mobility with a limbed robot," in *Intelligent Robots and Systems (IROS 2014), 2014 IEEE/RSJ International Conference on*, pp. 2341–2348, IEEE, 2014.

[22] A. Parness, "Testing gecko-like adhesives aboard the international space station," *Nature Scientific Reports*, p. in review, 2016.

[23] A Parness et al., "Gravity-independent rock climbing robot and sample acquisition tool with microspine grippers," *Journal of Field Robotics*, vol. 30, no. 6, pp. 897–915, 2013.

[24] R. Diankov, *Automated Construction of Robotic Manipulation Programs*. PhD thesis, Carnegie Mellon University, Robotics Institute, August 2010.

[25] K. Uckert et al., "Near-ir reflectance spectroscopy in a lava tube cave from a robotic platform," in *Lunar and Planetary Science Conference*, vol. 47, p. 2671, 2016.

[26] S. Kim, M. Spenko, S. Trujillo, B. Heyneman, V. Mattoli, and M. Cutkosky, "Whole body adhesion: hierarchical, directional and distributed control of adhesive forces for a climbing robot," *Robotics and Automation, 2007 IEEE International Conference on*, pp. 1268–1273, 2007.

[27] S. Kim, M. Spenko, S. Trujillo, B. Heyneman, D. Santos, and M. Cutkosky, "Smooth vertical surface climbing with directional adhesion," *Robotics, IEEE Transactions on*, vol. 24, no. 1, pp. 65 – 74, 2008.

[28] E. Hawkes, E. Eason, A. Asbeck, and M. Cutkosky, "The gecko's toe: Scaling directional adhesives for climbing applications," *IEEE/ASME Transactions on Mechatronics*, 2012.

[29] A. Parness et al., "A microfabricated wedge-shaped adhesive array displaying gecko-like dynamic adhesion, directionality and long lifetime," *Journal of the Royal Society, Interface*, vol. 6, pp. 1223–1232, Mar 2009.

[30] H. Jiang et al., "Scaling controllable adhesives to grapple floating objects in space," in *2015 IEEE International Conference on Robotics and Automation (ICRA)*, pp. 2828–2835, IEEE, 2015.

[31] A. T. Asbeck, S. Kim, M. R. Cutkosky, W. R. Provancher, and M. Lanzetta, "Scaling hard vertical surfaces with compliant microspine arrays," *Int J Robot Res*, vol. 25, no. 12, pp. 1165–1179, 2006.

[32] A. Parness, "Anchoring foot mechanisms for sampling and mobility in microgravity," *IEEE ICRA*, 2011.

[33] S. Kim, A. Asbeck, M. Cutkosky, and W. Provancher, "Spinybot II: climbing hard walls with compliant microspines," *Advanced Robotics, 2005. ICAR '05. Proceedings., 12th International Conference on*, pp. 601 – 606, Jun 2005.

[34] M. Spenko, G. Haynes, J. Saunders, M. Cutkosky, and A. Rizzi, "Biologically inspired climbing with a hexapedal robot," *Journal of Field Robotics*, Jan 2008.